Figure of merit for dark energy constraints from current observational data

Yun Wang*

Homer L. Dodge Department of Physics & Astronomy, University of Oklahoma, 440 West Brooks Street, Norman, Oklahoma 73019, USA

(Received 1 April 2008; published 18 June 2008)

In order to make useful comparisons of different dark energy experiments, it is important to choose the appropriate figure of merit (FoM) for dark energy constraints. Here we show that for a set of dark energy parameters $\{f_i\}$, it is most intuitive to define FoM $= 1/\sqrt{\det \mathrm{Cov}(f_1, f_2, f_3, \ldots)}$, where $\mathrm{Cov}(f_1, f_2, f_3, \ldots)$ is the covariance matrix of $\{f_i\}$. In order for this FoM to represent the dark energy constraints in an optimal manner, the dark energy parameters $\{f_i\}$ should have clear physical meaning and be minimally correlated. We demonstrate two useful choices of $\{f_i\}$ using 182 SNe Ia (from the HST/GOODS program, the first year Supernova Legacy Survey, and nearby SN Ia surveys), $[R(z_*), l_a(z_*), \Omega_b h^2]$ from the five year Wilkinson Microwave Anisotropy Probe observations, and Sloan Digital Sky Survey measurement of the baryon acoustic oscillation scale, assuming the Hubble Space Telescope prior of $H_0 = 72 \pm 8$ (km/s) Mpc^{-1}, and without assuming spatial flatness. We find that for a dark energy equation of state linear in the cosmic scale factor a, the correlation of $(w_0, w_{0.5})$ [$w_0 = w_X(z = 0)$, $w_{0.5} = w_X(z = 0.5)$, with $w_X(a) = 3w_{0.5} - 2w_0 + 3(w_0 - w_{0.5})a$] is significantly smaller than that of (w_0, w_a) [with $w_X(a) = w_0 + (1 - a)w_a$]. In order to obtain model-independent constraints on dark energy, we parametrize the dark energy density function $X(z) = \rho_X(z)/\rho_X(0)$ as a free function with $X_{0.5}$, $X_{1.0}$, and $X_{1.5}$ [values of $X(z)$ at $z = 0.5$, 1.0, and 1.5] as free parameters estimated from data. If one assumes a linear dark energy equation of state, current observational data are consistent with a cosmological constant at 68% C.L. If one assumes $X(z)$ to be a free function parametrized by $(X_{0.5}, X_{1.0}, X_{1.5})$, current data deviate from a cosmological constant at $z = 1$ at 68% C.L., but are consistent with a cosmological constant at 95% C.L. Future dark energy experiments will allow us to dramatically increase the FoM of constraints on $(w_0, w_{0.5})$, and of $(X_{0.5}, X_{1.0}, X_{1.5})$. This will significantly shrink the dark energy parameter space to either enable the discovery of dark energy evolution, or the conclusive evidence for a cosmological constant.

DOI: 10.1103/PhysRevD.77.123525 PACS numbers: 98.80.Es, 98.80.Jk

I. INTRODUCTION

The understanding of dark energy, the unknown cause for the observed cosmic acceleration [1,2], continues to be one of the most important challenges in cosmology today. Dark energy could be an unknown energy component [3–8], or a modification of general relativity [9–13]. References [14,15] contain reviews of many models. Much work continues to be done on the theoretical front, see, for example, [16–21]. Current observational data do not provide stringent constraints on dark energy, and allow a wide range of possibilities including dark energy being a cosmological constant (see, for example, [22–49]).

Future dark energy experiments that are significantly more ambitious than current ones are required to illuminate the nature of dark energy. In order to compare proposed future dark energy experiments in a useful manner, we need to choose the appropriate figure of merit (FoM) for dark energy constraints [50].

In this paper, we explore the optimization of FoM using current observational data from supernovae, galaxy clustering, and cosmic microwave background anisotropy (CMB) data. We describe our method in Sec. II, present our results in Sec. III, and conclude in Sec. IV.

II. METHOD

A. General definition for figure of merit

When we estimate a set of parameters, $\{f_i\}$ $(i = 1, 2, \ldots, N)$, from data, the most intuitive figure of merit is the N-dimensional volume enclosed by the 68% or 95% confidence level (C.L.) contours of the parameters. If the likelihood surfaces for all the parameters are Gaussian, this N-dimensional volume is proportional to the square root of the covariance matrix of $\{f_i\}$, $\sqrt{\det \mathrm{Cov}(f_1, f_2, f_3, \ldots)}$. For $N = 2$, the 68% or 95% C.L. contours of f_1 and f_2 are ellipses, with the enclosed area given by $\pi\sqrt{\det \mathrm{Cov}(f_1, f_2)}$ multiplied by 2.30 or 6.17. Parametrizing the dark energy equation of state as $w_X(a) = w_0 + (1 - a)w_a$ [51], the Dark Energy Task Force (DETF) defined FoM to be the inverse of the area enclosed by the 95% C.L. contour of (w_0, w_a) [52], i.e.,

$$\mathrm{FoM}_{\mathrm{DETF}} = \frac{1}{6.17\pi\sigma(w_a)\sigma(w_p)} \quad (1)$$

*wang@nhn.ou.edu

 © 2008 The American Physical Society

where $w_p = w_0 - w_a\langle\delta w_0 \delta w_a\rangle/\langle\delta w_a^2\rangle$, and $\sigma(w_i) = \sqrt{\langle\delta w_i^2\rangle}$. Note that $\sigma(w_a)\sigma(w_p) = \sqrt{\mathrm{detCov}(w_0, w_a)}$, thus the conversion to w_p is *not* needed to calculate the FoM.

For real data, the likelihood surfaces for the parameters $\{f_i\}$ are almost always *non-Gaussian* at the 95% C.L., thus defining the FoM as an enclosed area or volume by the 95% C.L. contours of $\{f_i\}$ becomes problematic. We propose the definition for a relative generalized FoM given by

$$\mathrm{FoM}_r = \frac{1}{\sqrt{\mathrm{detCov}(f_1, f_2, f_3, \ldots)}}, \tag{2}$$

where $\{f_i\}$ are the chosen set of dark energy parameters. This definition has the advantage of being easy to calculate for either real or simulated data. We have streamlined the definition to omit numerical factors since what matters is the relative FoM between different experiments.

Note that while this FoM definition has an intuitive physical interpretation, it rewards experiments that yield very correlated estimates of the dark energy parameters. This is especially true in applying the DETF FoM, since (w_0, w_a) are always highly correlated. Hence the dark energy FoM [as defined in Eq. (2)] is most meaningful when the dark energy parameters $\{f_i\}$ are chosen such that they are minimally correlated with each other.

B. Dark energy parametrization

We study constraints on a two-parameter dark energy equation of state $w_X(z)$ linear in a, as well as the dark energy density function $X(z) \equiv \rho_X(z)/\rho_X(0)$ as a free function at $z \leq 1.5$.

The two-parameter $w_X(z)$ is given by

$$\begin{aligned} w_X(a) &= \left(\frac{a_c - a}{a_c - 1}\right)w_0 + \left(\frac{a - 1}{a_c - 1}\right)w_c \\ &= \frac{a_c w_0 - w_c + a(w_c - w_0)}{a_c - 1} \end{aligned} \tag{3}$$

where $w_0 = w_X(z = 0)$, and $w_c = w_X(z = z_c)$. Equation (3) corresponds to a dark energy density function

$$\begin{aligned} X(z) = \exp\Bigg\{3\left[1 + \left(\frac{a_c w_0 - w_c}{a_c - 1}\right)\right]\ln(1 + z) \\ + 3\left(\frac{w_c - w_0}{a_c - 1}\right)\frac{z}{1 + z}\Bigg\}. \end{aligned} \tag{4}$$

Equation (3) is related to $w_X(z) = w_0 + (1 - a)w_a$ by setting

$$w_a = \frac{w_c - w_0}{1 - a_c}, \quad \text{or} \quad w_c = w_0 + (1 - a_c)w_a. \tag{5}$$

If we choose $a_c = 1 + \sigma^2(w_0)/\sigma^2(w_0 w_a)$, then (w_0, w_c) are *uncorrelated*. For current data, $z_c \sim 0.3$. Choosing a_c to make (w_0, w_c) uncorrelated has the disadvantage that a_c is different for different data sets.

We recommend choosing $z_c = 0.5$; it is sufficiently close to $z_c \sim 0.3$ that the correlation of w_0 and $w_{0.5} = w_X(z = 0.5)$ is relatively small. It is straightforward to show that if $|\sigma^2(w_0 w_a)/[\sigma(w_0)\sigma(w_a)]| < 1$, (w_0, w_c) are *less* correlated than (w_0, w_a) if

$$\sigma^2(w_0) < 2|(1 - a_c)\sigma^2(w_0 w_a)|. \tag{6}$$

This is always satisfied for $z_c = 0.5$. Choosing $z_c = 0.5$, the correlation of $(w_0, w_{0.5})$ is smaller than that of (w_0, w_a) by about a factor of 2 for the combined SNe, baryon acoustic oscillation (BAO), and CMB data considered in this paper. Fixing z_c has the significant advantage of allowing the comparison of the *same* dark energy property for different data sets. For our results for the two-parameter dark energy model, we use Eq. (3) with $a_c = 1/(1 + 0.5) = 2/3$ ($z_c = 0.5$). Thus

$$\begin{aligned} w_X(a) &= 3w_{0.5} - 2w_0 + 3(w_0 - w_{0.5})a \\ X(z) &= (1 + z)^{3(1 - 2w_0 + 3w_{0.5})}\exp\left[9(w_0 - w_{0.5})\frac{z}{1 + z}\right]. \end{aligned} \tag{7}$$

In order to obtain model-independent constraints on dark energy, we parametrize the dark energy density function $X(z) = \rho_X(z)/\rho_X(0)$ as a free functions with $X_{0.5}$, $X_{1.0}$, and $X_{1.5}$ [values of $X(z)$ at $z = 0.5$, 1.0, and 1.5] as free parameters estimated from data. At $z > 1.5$, we choose either $X(z) = X_{1.5}$ or $X(z) = X_{1.5}e^{\alpha(z - 1.5)}$ (with α as an additional parameter to be estimated from data). Our results are insensitive to the assumption about $X(z)$ at $z > 1.5$ (other than that dark energy becomes insignificant at $z > 1.5$). As more data become available at $z > 1.5$, we can include $X_{2.0} = X(z = 2.0)$, $X_{2.5} = X(z = 2.5)$, and $X_{3.0} = X(z = 3.0)$ as estimated parameters, as well as inserting more estimated $X(z)$ values at $z < 1.5$. Early dark energy (significant at high z) is not required by current data, and leads to contradiction with observed cosmic structure formation [53], unless a cutoff is imposed.

The constraints on $X_{0.5}$, $X_{1.0}$, and $X_{1.5}$ are insensitive to the interpolation used in deriving $X(z)$ elsewhere. The simplest smooth interpolation is given by a polynomial

$$\begin{aligned} X(z) = &-\tfrac{1}{2}(3\bar{z} - 1)(3\bar{z} - 2)(\bar{z} - 1) + \tfrac{9}{2}X_{0.5}\bar{z}(3\bar{z} - 2)(\bar{z} - 1) \\ &- \tfrac{9}{2}X_{1.0}\bar{z}(3\bar{z} - 1)(\bar{z} - 1) + \tfrac{1}{2}X_{1.5}\bar{z}(3\bar{z} - 1)(3\bar{z} - 2), \end{aligned} \tag{8}$$

where $\bar{z} = z/1.5$.

C. Data analysis technique

The comoving distance from the observer to redshift z is given by

$$r(z) = cH_0^{-1}|\Omega_k|^{-1/2}\mathrm{sinn}[|\Omega_k|^{1/2}\Gamma(z)],$$
$$\Gamma(z) = \int_0^z \frac{dz'}{E(z')}, \qquad E(z) = H(z)/H_0 \tag{9}$$

where $\Omega_k = -k/H_0^2$ with k denoting the curvature constant, and $\mathrm{sinn}(x) = \sin(x), x, \sinh(x)$ for $\Omega_k < 0$, $\Omega_k = 0$, and $\Omega_k > 0$ respectively, and

$$E^2(z) = \Omega_m(1+z)^3 + \Omega_{\rm rad}(1+z)^4 + \Omega_k(1+z)^2 + \Omega_X X(z) \tag{10}$$

with $\Omega_X = 1 - \Omega_m - \Omega_{\rm rad} - \Omega_k$, and the dark energy density function $X(z) \equiv \rho_X(z)/\rho_X(0)$.

CMB data give us the comoving distance to the photon-decoupling surface $r(z_*)$, and the comoving sound horizon at photon-decoupling epoch [54,55]

$$r_s(z_*) = \int_0^{t_*} \frac{c_s dt}{a} = cH_0^{-1}\int_{z_*}^{\infty} dz \frac{c_s}{E(z)} = cH_0^{-1}\int_0^{a_*} \frac{da}{\sqrt{3(1+\bar{R}_b a)a^4 E^2(z)}}, \tag{11}$$

where a is the cosmic scale factor, $a_* = 1/(1+z_*)$, and $a^4E^2(z) = \Omega_m(a + a_{\rm eq}) + \Omega_k a^2 + \Omega_X X(z)a^4$, with $a_{\rm eq} = \Omega_{\rm rad}/\Omega_m = 1/(1+z_{\rm eq})$, and $z_{\rm eq} = 2.5\times 10^4 \Omega_m h^2 (T_{\rm CMB}/2.7\ {\rm K})^{-4}$. The sound speed is $c_s = 1/\sqrt{3(1+\bar{R}_b a)}$, with $\bar{R}_b a = 3\rho_b/(4\rho_\gamma)$, $\bar{R}_b = 31500\Omega_b h^2 (T_{\rm CMB}/2.7\ {\rm K})^{-4}$. Cosmic Background Explorer four year data give $T_{\rm CMB} = 2.728 \pm 0.004$ K (95% C.L.) [56]. We take $T_{\rm CMB} = 2.725$ following [57], since we will use the CMB bounds derived by [57]. The angular scale of the sound horizon at recombination is defined as $l_a = \pi r(z_*)/r_s(z_*)$ [55].

Wang and Mukherjee [58] showed that the CMB shift parameters

$$R \equiv \sqrt{\Omega_m H_0^2}\, r(z_*), \qquad l_a \equiv \pi r(z_*)/r_s(z_*), \tag{12}$$

together with $\Omega_b h^2$, provide an efficient summary of CMB data as far as dark energy constraints go. We use the covariance matrix of $[R(z_*), l_a(z_*), \Omega_b h^2]$ from the five year WMAP data (Table 11 of [57]), with z_* given by fitting formulas from Hu and Sugiyama [59]

$$z_* = 1048[1 + 0.00124(\Omega_b h^2)^{-0.738}][1 + g_1(\Omega_m h^2)^{g_2}], \tag{13}$$

where

$$g_1 = \frac{0.0783(\Omega_b h^2)^{-0.238}}{1 + 39.5(\Omega_b h^2)^{0.763}} \tag{14}$$

$$g_2 = \frac{0.560}{1 + 21.1(\Omega_b h^2)^{1.81}}. \tag{15}$$

CMB data are included in our analysis by adding the following term to the χ^2 of a given model with $p_1 = R(z_*)$, $p_2 = l_a(z_*)$, and $p_3 = \Omega_b h^2$:

$$\chi^2_{\rm CMB} = \Delta p_i [{\rm Cov}^{-1}(p_i, p_j)]\Delta p_j, \qquad \Delta p_i = p_i - p_i^{\rm data}, \tag{16}$$

where $p_i^{\rm data}$ are the maximum likelihood values given in Table 10 of [57].

SN Ia data give the luminosity distance as a function of redshift, $d_L(z) = (1+z)r(z)$. We use 182 SNe Ia from the Hubble Space Telescope (HST)/GOODS program [60] and the first year Supernova Legacy Survey [61], together with nearby SN Ia data, as compiled by [60]. We do not include the ESSENCE data [62], as these are not yet derived using the same method as those used in [60]. Combining SN Ia data derived using different analysis techniques leads to systematic effects in the estimated SN distance moduli [62,63]. Appendix A of [58] describes in detail how we use SN Ia data (flux averaged to reduce lensinglike systematic effects [63–65] and marginalized over H_0) in this paper.

We also use the Sloan Digital Sky Survey (SDSS) BAO scale measurement by adding the following term to the χ^2 of a model:

$$\chi^2_{\rm BAO} = \left[\frac{(A - A_{\rm BAO})}{\sigma_A}\right]^2, \tag{17}$$

where A is defined as

$$A = \left[r^2(z_{\rm BAO})\frac{cz_{\rm BAO}}{H(z_{\rm BAO})}\right]^{1/3}\frac{(\Omega_m H_0^2)^{1/2}}{cz_{\rm BAO}}, \tag{18}$$

and $A_{\rm BAO} = 0.469(n_S/0.98)^{-0.35}$, $\sigma_A = 0.017$, and $z_{\rm BAO} = 0.35$ (independent of a dark energy model) [66]. We take the scalar spectral index $n_S = 0.96$ as measured by the WMAP five year observations [57].

For Gaussian distributed measurements, the likelihood function $L \propto e^{-\chi^2/2}$, with

$$\chi^2 = \chi^2_{\rm CMB} + \chi^2_{\rm SNe} + \chi^2_{\rm BAO}, \tag{19}$$

where $\chi^2_{\rm CMB}$ is given in Eq. (16), $\chi^2_{\rm SNe}$ is given in Appendix A of [58], and $\chi^2_{\rm BAO}$ is given in Eq. (17).

The current big bang nucleosynthesis (BBN) constraints [67], $S = 0.942 \pm 0.030$ ($N_\nu = 2.30^{+0.35}_{-0.34}$) rule out the standard model of particle physics ($S = 1$, $N_\nu = 3$) at 1σ [67]. Given the uncertainties involved in deriving the BBN constraints, we relax the standard deviation of S by a factor of 2, so that the standard model of particle physics is allowed at 1σ. We find that the resultant BBN constraints do not have measurable effect on our dark energy constraints.

For all the dark energy constraints from combining the different data sets presented in this paper, we marginalize the SN Ia data over H_0 in flux-averaging statistics [58], and impose a prior of $H_0 = 72 \pm 8$ (km/s) Mpc^{-1} from the HST Cepheid variable star observations [68].

We run a Monte Carlo Markov Chain (MCMC) based on the MCMC engine of [69] to obtain $\mathcal{O}(10^6)$ samples for each set of results presented in this paper. The parameters

used are $(\Omega_k, \Omega_m, h, \Omega_b h^2, \mathbf{p}_{\rm DE})$. The dark energy parameter set is described in Sec. II B. We assumed flat priors for all the parameters, and allowed ranges of the parameters wide enough such that further increasing the allowed ranges has no impact on the results. The chains typically have worst e-values [the variance(mean)/mean(variance) of 1/2 chains] much smaller than 0.005, indicating convergence. The chains are subsequently appropriately thinned to ensure independent samples.

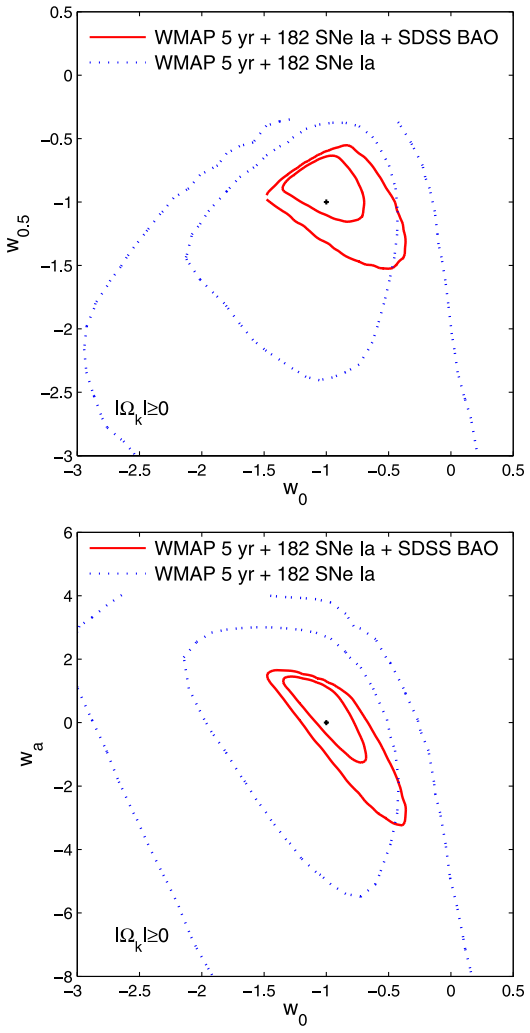

FIG. 1 (color online). The 68% and 95% C.L. contours of $(w_0, w_{0.5})$ (upper panel) and (w_0, w_a) (lower panel) from the WMAP five year measurement of $[R(z_*), l_a(z_*), \Omega_b h^2]$, and 182 SNe Ia (from the HST/GOODS program, the first year Supernova Legacy Survey, and nearby SN Ia surveys), with and without the SDSS measurement of the BAO scale.

III. RESULTS

Figure 1 shows the 68% and 95% C.L. contours of $(w_0, w_{0.5})$ (upper panel) and (w_0, w_a) (lower panel) from the WMAP 5 year measurement of $[R(z_*), l_a(z_*), \Omega_b h^2]$, and 182 SNe Ia (from the HST/GOODS program, the first year Supernova Legacy Survey, and nearby SN Ia surveys), with and without the SDSS measurement of the BAO scale. We have assumed the HST prior of $H_0 = 72 \pm 8$ (km/s) Mpc^{-1}, and allowed Ω_k to vary. Table I shows the mean, rms variance, and correlation coefficients of $(w_0, w_{0.5})$ and (w_0, w_a), as well as the relative dark energy FoM$_r$ defined in Eq. (2). Note that Pearson's correlation coefficient $\rho_{xy} = \sigma^2(xy)/[\sigma(x)\sigma(y)]$. Adding the SDSS BAO scale measurement improves the FoM$_r$ by a factor of 21.5 for $(w_0, w_{0.5})$, and by a factor of 27.0 for (w_0, w_a). Since $(w_0, w_{0.5})$ are significantly less correlated than (w_0, w_a), the improvement factor in FoM$_r$ of $(w_0, w_{0.5})$ is a more reliable indicator of the impact of adding the SDSS BAO scale measurement.

Figure 2 shows the one dimensional marginalized probability distributions (pdf) of $(\Omega_m, h, \Omega_k, \Omega_b h^2, w_0, w_a)$, for 182 SNe Ia, the SDSS BAO scale measurement, and the WMAP five year data in the form of measured (1) $[R(z_*), l_a(z_*), \Omega_b h^2]$ (solid lines), (2) $[R(z_*), l_a(z_*), \Omega_b h^2]$ with z_* fixed at 1090.4 (dotted lines), and (3) $[R(z_*), l_a(z_*), z_*]$ (dashed lines). For reference, the dot-dashed line shows the pdfs for 182 SNe Ia, the SDSS measurement of the BAO scale, and the WMAP three year data in the form of measured $[R(z_{\rm CMB}), l_a(z_{\rm CMB}), \Omega_b h^2]$ with $z_{\rm CMB}$ fixed at 1089 from [58].

We find that in spite of the different pdfs for $\Omega_b h^2$, using the $[R(z_*), l_a(z_*), \Omega_b h^2]$ and $[R(z_*), l_a(z_*), z_*]$ measurements give about the same constraints on $(\Omega_m, h, \Omega_k, w_0, w_a)$. Using the $[R(z_*), l_a(z_*), \Omega_b h^2]$ measurement with z_* fixed at 1090.4 gives slightly tighter constraints on (w_0, w_a). In combination with the supernova and BAO data, the WMAP five year data improve constraints on (w_0, w_a) slightly compared to the WMAP three year data, while tightening the constraints on Ω_k and h.

Figure 3 shows the constraints on the dark energy density function $X(z) = \rho_X(z)/\rho_X(0)$ parametrized by Eq. (8),

TABLE I. Constraints on $(w_0, w_{0.5})$ and (w_0, w_a).

Data	$\mu(w_0)$	$\sigma(w_0)$	$\mu(w_0)$	$\sigma(w_{0.5})$	$\rho_{w_0 w_{0.5}}$	FoM$_r$
WMAP5 + SNe	−1.075	0.598	−1.939	1.572	−0.401	1.163
WMAP5 + SNe + BAO	−0.937	0.226	−0.953	0.206	−0.512	25.013
Data	$\mu(w_0)$	$\sigma(w_0)$	$\mu(w_a)$	$\sigma(w_a)$	$\rho_{w_0 w_a}$	FoM$_r$
WMAP5 + SNe	−1.073	0.647	−2.960	6.759	−0.670	0.308
WMAP5 + SNe + BAO	−0.938	0.226	−0.045	1.126	−0.882	8.326

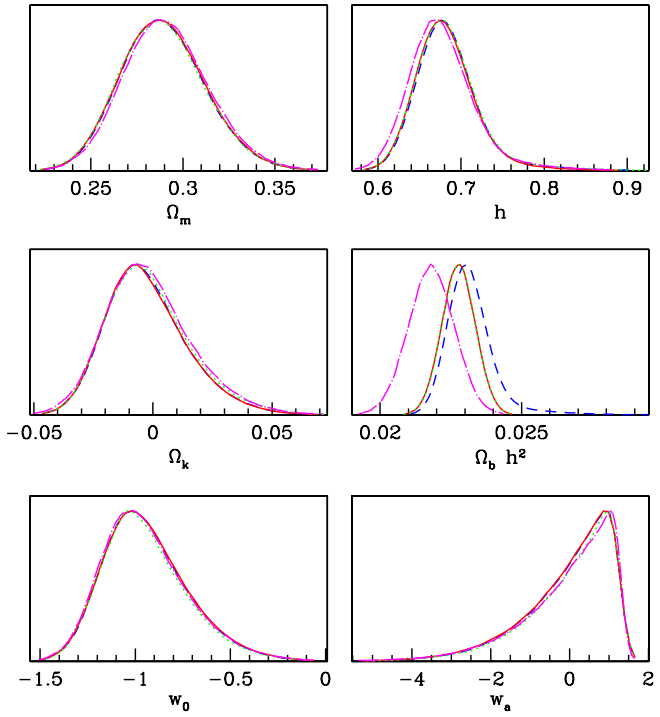

FIG. 2 (color online). One dimensional marginalized pdfs of $(\Omega_m, h, \Omega_k, \Omega_b h^2, w_0, w_a)$ from 182 SNe Ia, the SDSS BAO scale measurement, and the WMAP five year data in the form of measured (1) $[R(z_*), l_a(z_*), \Omega_b h^2]$ (solid lines), (2) $[R(z_*), l_a(z_*), \Omega_b h^2]$ with z_* fixed at 1090.4 (dotted lines), and (3) $[R(z_*), l_a(z_*), z_*]$ (dashed lines). The dot-dashed line shows the pdfs for 182 SNe Ia, the SDSS measurement of the BAO scale, and the WMAP three year data in the form of measured $[R(z_{\rm CMB}), l_a(z_{\rm CMB}), \Omega_b h^2]$ with $z_{\rm CMB}$ fixed at 1089 from [58].

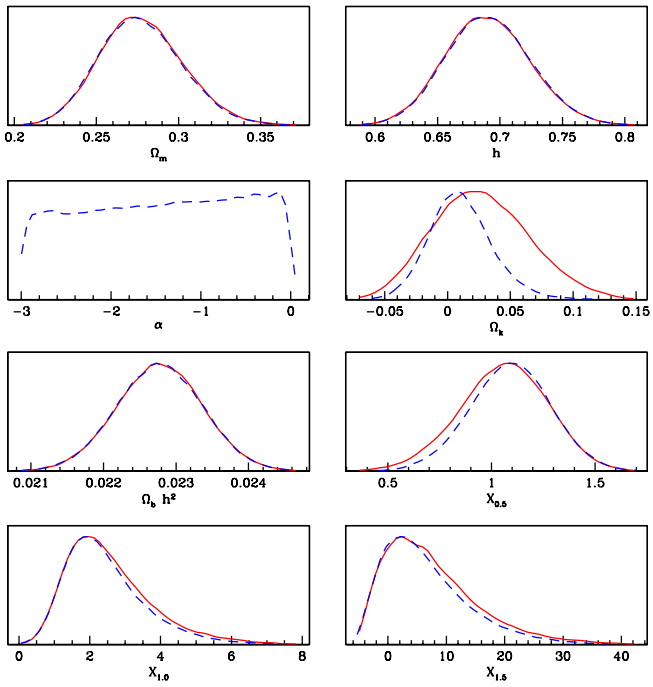

FIG. 3 (color online). One dimensional marginalized pdfs of dark energy and cosmological parameters from the WMAP five year measurement of $[R(z_*), l_a(z_*), \Omega_b h^2]$, 182 SNe Ia, and the SDSS BAO scale measurement. Solid and dashed lines indicate $X(z)$ at $z > 1.5$ given by $X(z) = X_{1.5}$ and $X(z) = X_{1.5}\exp[\alpha(z-1.5)]$, respectively.

with $X(z)$ at $z > 1.5$ given by either $X(z) = X_{1.5}$ or $X(z) = X_{1.5}\exp[\alpha(z-1.5)]$. Note that the assumption about dark energy at $z > 1.5$ has only a weak effect on the dark energy constraints at $z \leq 1.5$. Note that taking $X(z > 1.5) = X_{1.5}$ gives slightly less stringent constraints on dark energy at $z \leq 1.5$. This is because parametrizing dark energy at $z > 1.5$ with an extra parameter requires choosing the early dark energy parametrization such that it is not degenerate with cosmic curvature; this is why Ω_k is not well constrained if we choose $X(z > 1.5) = X_{1.5}(1+z)^\alpha$, but Ω_k is well constrained if we choose $X(z > 1.5) = X_{1.5}\exp[\alpha(z-1.5)]$ [58]. The latter helps break the degeneracy of Ω_k with $X(z)$, thus leading to much tighter constraints on Ω_k and slightly tighter constraints on $X(z)$ at $z \leq 1.5$ (see Fig. 3). This suggests that the more conservative approach in constraining dark energy is to assume that $X(z > 1.5) = X_{1.5}$.

Table II shows the mean, rms variance, and correlation coefficients of $(X_{0.5}, X_{1.0}, X_{1.5})$, as well as the relative dark energy FoM$_r$ defined in Eq. (2).

IV. SUMMARY AND DISCUSSION

In order to compare current and future dark energy experiments on the same footing, we have introduced a simple and straightforward definition for the FoM of constraints on any set of dark energy parameters, Eq. (2), that is easily applicable to both real and simulated data.

We recommend the adoption of two dark energy parametrizations in comparing different experiments: (1) A dark energy equation of state $w_X(z)$ linear in a, with its values at $z = 0$ and $z = 0.5$, $(w_0, w_{0.5})$, as parameters estimated from data [see Eq. (7)]. We find that $(w_0, w_{0.5})$ are significantly less correlated than (w_0, w_a) (see Table I

TABLE II. Constraints on $X(z)$ parametrized by $(X_{0.5}, X_{1.0}, X_{1.5})$.

$X(z > 1.5)$	$\mu(X_{0.5})$	$\sigma(X_{0.5})$	$\mu(X_{1.0})$	$\sigma(X_{1.0})$	$\mu(X_{1.5})$	$\sigma(X_{1.5})$	$\rho_{X_{0.5}X_{1.0}}$	$\rho_{X_{0.5}X_{1.5}}$	$\rho_{X_{1.0}X_{1.5}}$	FoM$_r$
$X_{1.5}$	1.059	0.213	2.556	1.215	7.503	8.037	−0.389	−0.666	0.906	2.077
$X_{1.5}e^{\alpha(z-1.5)}$	1.091	0.195	2.436	1.121	6.533	7.351	−0.303	−0.609	0.895	2.402

and Fig. 1), hence the factor of improvement in the FoM$_r$ [as defined in Eq. (2)] for $(w_0, w_{0.5})$ is a more reliable indicator of the improvement in dark energy constraints than the factor of improvement of FoM$_r$ for (w_0, w_a). (2) The dark energy density function $X(z) = \rho_X(z)/\rho_X(0)$ parametrized by its values at $z = 0.5$, 1.0, and 1.5, $(X_{0.5}, X_{1.0}, X_{1.5})$, for $z \leq 1.5$ [see Eq. (8)], and $X(z > 1.5) = X_{1.5}$. We find that this flat cutoff in $X(z)$ gives more conservative constraints on $X(z)$ than parametrizing early dark energy with an extra parameter such that cosmic curvature is constrained (see Fig. 3).

We have demonstrated the use of the FoM$_r$ [see Eq. (2)] for these two dark energy parametrizations [see Eqs. (7) and (8)] using the WMAP five year measurement of $[R(z_*), l_a(z_*), \Omega_b h^2]$, 182 SNe Ia (from the HST/GOODS program, the first year Supernova Legacy Survey, and nearby SN Ia surveys), and the SDSS measurement of the BAO scale (see Figs. 1–3). Dark energy is consistent with a cosmological constant at 68% C.L. if one assumes the two-parameter dark energy equation of state model, $w_X(a) = 3w_{0.5} - 2w_0 + 3(w_0 - w_{0.5})a$. If one assumes dark energy density to be a free function parametrized by its values at $z = 0.5$, 1.0, and 1.5, then dark energy deviates from a cosmological constant at $z = 1.0$ at 68% C.L., but is consistent with a cosmological constant at 95% C.L. (see Fig. 3). This illustrates the importance of using the model-independent parametrization in probing dark energy. Measuring $X(z)$ as a free function from data allows us to detect epochs of variation in dark energy density [70–72]. It also allows us to constrain a broader class of dark energy models than represented by $w_X(z)$; for example, dark energy models in which $X(z)$ becomes negative in the past or future, which are excluded by fiat if one only measures $w_X(z)$ since $X(z) = \exp\{\int_0^z dz' 3[1 + w_X(z')]/(1 + z')\}$ [23]. The two-parameter dark energy equation of state model (linear in a) implies strong assumptions about dark energy, and is not sensitive to a transient variation in dark energy; thus it is most useful in comparing forecasts for future dark energy experiments under the simplest assumptions.

Future dark energy experiments from both ground and space [52,73–77], together with CMB data from Planck [78], will dramatically improve our ability to probe dark energy, and eventually shed light on the nature of dark energy. Using both a linear dark energy equation of state [parameterized by $(w_0, w_{0.5})$] and dark energy density function $X(z)$ as a free function [parametrized by $(X_{0.5}, X_{1.0}, X_{1.5})$] provides a simple and balanced approach to exploring dark energy. Proposed future dark energy experiments should be evaluated by comparing their FoM$_r$ for both $(w_0, w_{0.5})$ and $(X_{0.5}, X_{1.0}, X_{1.5})$ to that of current data.

ACKNOWLEDGMENTS

I am grateful to Eiichiro Komatsu for sending me the covariance matrix for $[R(z_*), l_a(z_*), z_*, \Omega_b h^2]$ from the WMAP five year data, and for helpful discussions. I acknowledge the use of COSMOMC in processing the MCMC chains.

[1] A. G. Riess *et al.*, Astron. J. **116**, 1009 (1998).
[2] S. Perlmutter *et al.*, Astrophys. J. **517**, 565 (1999).
[3] K. Freese, F. C. Adams, J. A. Frieman, and E. Mottola, Nucl. Phys. **B287**, 797 (1987).
[4] A. D. Linde, in *Three Hundred Years of Gravitation*, edited by S. W. Hawking and W. Israel (Cambridge University Press, Cambridge, England, 1987), pp. 604–630.
[5] P. J. E. Peebles and B. Ratra, Astrophys. J. **325**, L17 (1988).
[6] C. Wetterich, Nucl. Phys. **B302**, 668 (1988).
[7] J. A. Frieman, C. T. Hill, A. Stebbins, and I. Waga, Phys. Rev. Lett. **75**, 2077 (1995).
[8] R. Caldwell, R. Dave, and P. J. Steinhardt, Phys. Rev. Lett. **80**, 1582 (1998).
[9] V. Sahni and S. Habib, Phys. Rev. Lett. **81**, 1766 (1998).
[10] L. Parker and A. Raval, Phys. Rev. D **60**, 063512 (1999).
[11] B. Boisseau, G. Esposito-Farèse, D. Polarski, and A. A. Starobinsky, Phys. Rev. Lett. **85**, 2236 (2000).
[12] G. Dvali, G. Gabadadze, and M. Porrati, Phys. Lett. B **485**, 208 (2000).
[13] K. Freese and M. Lewis, Phys. Lett. B **540**, 1 (2002).
[14] T. Padmanabhan, Phys. Rep. **380**, 235 (2003).
[15] P. J. E. Peebles and B. Ratra, Rev. Mod. Phys. **75**, 559 (2003).
[16] V. K. Onemli and R. P. Woodard, Phys. Rev. D **70**, 107301 (2004).
[17] V. F. Cardone, C. Tortora, A. Troisi, and S. Capozziello, Phys. Rev. D **73**, 043508 (2006).
[18] R. R. Caldwell, W. Komp, L. Parker, and D. A. T. Vanzella, Phys. Rev. D **73**, 023513 (2006).
[19] E. O. Kahya and V. K. Onemli, Phys. Rev. D **76**, 043512 (2007).
[20] A. De Felice, P. Mukherjee, and Y. Wang, Phys. Rev. D **77**, 024017 (2008).
[21] T. Koivisto and D. F. Mota, Phys. Rev. D **75**, 023518 (2007).
[22] Y. Wang, J. M. Kratochvil, A. Linde, and M. Shmakova, J. Cosmol. Astropart. Phys. 12 (2004) 006.
[23] Y. Wang and M. Tegmark, Phys. Rev. Lett. **92**, 241302 (2004).
[24] Y. Wang and M. Tegmark, Phys. Rev. D **71**, 103513 (2005).
[25] U. Alam and V. Sahni, Phys. Rev. D **73**, 084024 (2006).
[26] R. A. Daly and S. G. Djorgovski, arXiv:astro-ph/0512576.

[27] H. K. Jassal, J. S. Bagla, and T. Padmanabhan, Mon. Not. R. Astron. Soc. **356**, L11 (2005).
[28] D. Polarski and A. Ranquet, Phys. Lett. B **627**, 1 (2005).
[29] V. Barger, Y. Gao, and D. Marfatia, Phys. Lett. B **648**, 127 (2007).
[30] J. Dick, L. Knox, and M. Chu, J. Cosmol. Astropart. Phys. 07 (2006) 001.
[31] D. Huterer and H. V. Peiris, Phys. Rev. D **75**, 083503 (2007).
[32] K. Ichikawa, M. Kawasaki, T. Sekiguchi, and T. Takahashi, J. Cosmol. Astropart. Phys. 12 (2006) 005.
[33] H. K. Jassal, J. S. Bagla, and T. Padmanabhan, arXiv:astro-ph/0601389.
[34] A. R. Liddle, P. Mukherjee, D. Parkinson, and Y. Wang, Phys. Rev. D **74**, 123506 (2006).
[35] S. Nesseris and L. Perivolaropoulos, Phys. Rev. D **73**, 103511 (2006); J. Cosmol. Astropart. Phys. 02 (2007) 025.
[36] C. Schimd *et al.*, Astron. Astrophys. **463**, 405 (2007).
[37] L. Samushia and B. Ratra, Astrophys. J. **650**, L5 (2006).
[38] Y. Wang and P. Mukherjee, Astrophys. J. **650**, 1 (2006).
[39] K. M. Wilson, G. Chen, and B. Ratra, Mod. Phys. Lett. A **21**, 2197 (2006).
[40] J.-Q. Xia, G.-B. Zhao, H. Li, B. Feng, and X. Zhang, Phys. Rev. D **74**, 083521 (2006).
[41] U. Alam, V. Sahni, and A. A. Starobinsky, J. Cosmol. Astropart. Phys. 02 (2007) 011.
[42] C. Clarkson, M. Cortes, and B. A. Bassett, J. Cosmol. Astropart. Phys. 08 (2007) 011.
[43] T. M. Davis *et al.*, Astrophys. J. **666**, 716 (2007).
[44] Y. Gong and A. Wang, Phys. Rev. D **75**, 043520 (2007).
[45] K. Ichikawa and T. Takahashi, J. Cosmol. Astropart. Phys. 02 (2007) 001.
[46] H. Wei and S. N. Zhang, Phys. Lett. B **644**, 7 (2007).
[47] E. L. Wright, arXiv:astro-ph/0701584.
[48] J. Zhang, X. Zhang, and H. Liu, Mod. Phys. Lett. A **23**, 139 (2008).
[49] C. Zunckel and R. Trotta, Mon. Not. R. Astron. Soc. **380**, 865 (2007).
[50] A. Albrecht and G. Bernstein, Phys. Rev. D **75**, 103003 (2007); S. Sullivan *et al.*, arXiv:0709.1150.
[51] M. Chevallier and D. Polarski, Int. J. Mod. Phys. D **10**, 213 (2001).
[52] A. Albrecht, G. Bernstein, R. Cahn, W. L. Freedman, J. Hewitt, W. Hu, J. Huth, M. Kamionkowski, E. W. Kolb, L. Knox, J. C. Mather, S. Staggs, and N. B. Suntzeff, arXiv: astro-ph/0609591.
[53] H. Sandvik, M. Tegmark, M. Zaldarriaga, and I. Waga, Phys. Rev. D **69**, 123524 (2004).
[54] D. Eisenstein and W. Hu, Astrophys. J. **496**, 605 (1998).
[55] L. Page *et al.*, Astrophys. J. Suppl. Ser. **148**, 233 (2003).
[56] D. J. Fixsen, Astrophys. J. **473**, 576 (1996).
[57] E. Komatsu *et al.*, arXiv:0803.0547.
[58] Y. Wang and P. Mukherjee, Phys. Rev. D **76**, 103533 (2007).
[59] W. Hu and N. Sugiyama, Astrophys. J. **471**, 542 (1996).
[60] A. G. Riess *et al.*, Astrophys. J. **659**, 98 (2007).
[61] P. Astier*et al.*, Astron. Astrophys. **447**, 31 (2006).
[62] W. M. Wood-Vasey *et al.*, Astrophys. J. **666**, 694 (2007).
[63] Y. Wang, Astrophys. J. **536**, 531 (2000).
[64] Y. Wang and P. Mukherjee, Astrophys. J. **606**, 654 (2004).
[65] Y. Wang, J. Cosmol. Astropart. Phys. 03 (2005) 005.
[66] D. Eisenstein *et al.*, Astrophys. J. **633**, 560 (2005).
[67] G. Steigman, arXiv:astro-ph/0611209.
[68] W. L. Freedman *et al.*, Astrophys. J. **553**, 47 (2001).
[69] A. Lewis and S. Bridle, Phys. Rev. D **66**, 103511 (2002).
[70] Y. Wang and P. Garnavich, Astrophys. J. **552**, 445 (2001).
[71] M. Tegmark, Phys. Rev. D **66**, 103507 (2002).
[72] Y. Wang and K. Freese, Phys. Lett. B **632**, 449 (2006).
[73] Y. Wang, Astrophys. J. **531**, 676 (2000).
[74] See, for example, http://www.astro.ubc.ca/LMT/alpaca/; http://www.lsst.org/; http://www.as.utexas.edu/hetdex/. Reference [52] contains a more complete list of future dark energy experiments.
[75] Y. Wang *et al.*, Bull. Am. Astron. Soc. **36**, 1560 (2004); A. Crotts *et al.*, arXiv:astro-ph/0507043; E. Cheng and Y. Wang *et al.*, Proc. SPIE Int. Soc. Opt. Eng. **6265**, 626529 (2006); http://jedi.nhn.ou.edu/.
[76] M. Robberto, A Cimatti, and SPACE Science Team, arXiv:0710.3970 [Nuovo Cimento (to be published)].
[77] Y. Wang, arXiv:0710.3885.
[78] Planck Bluebook, http://www.rssd.esa.int/index.php?project=PLANCK.